CUED - Engineering Tripos Part IIB 2021-2022 **Module Coursework**

Module	4A7	Title of report	TRANSONIC AIRFOIL DESIGN

Date submitted: 09/11/2021	Assessment for this module is 100% coursework of which this assignment forms 50%

UNDERGRADUATE STUDENTS ONLY			**POST GRADUATE STUDENTS ONLY**			
Candidate number:	5726A		Name:		College:	

Feedback to the student ☐ **See also comments in the text**		Very good	**Good**	Needs improvmt
CONTENT	**Completeness, quantity of content:** Has the report covered all aspects of the lab? Has the analysis been carried out thoroughly?			
	Correctness, quality of content Is the data correct? Is the analysis of the data correct? Are the conclusions correct?			
	Depth of understanding, quality of discussion Does the report show a good technical understanding? Have all the relevant conclusions been drawn?			
	Comments:			
PRESENTATION	**Attention to detail, typesetting and typographical errors** Is the report free of typographical errors? Are the figures/tables/references presented professionally?			
	Comments:			

Marker: Date:

1. Summary

A supercritical transonic aerofoil is designed which maximises lift while satisfying the constraints on wave drag and boundary layer separation. Its performance is evaluated using a VGK solver at both design and off-design conditions by varying Mach number and incidence. Aerofoil improvements and limitations of VGK are discussed. An operation envelope has been found in which the choice of design point is questioned, using judgement to weigh up different indicators for the onset of shock-induced and trailing edge separation, buffeting and drag rise.

2. Design Point

Firstly, a Mach number of 0.73 and a Reynold's number of 9×10^6 were chosen. A larger Mach number moves the upper surface shock aft and strengthens it. This creates a larger wave drag. However, a high Mach number also leads to higher coefficient of lift (C_L), as the area between the upper and lower surface pressure distribution increases. As the objective is to maximise C_L while constraining to wave drag count limits, a compromise was made between lift and drag, hence the intermediate Mach number was chosen.

A good supercritical section requires a small leading-edge radius as that strengthens the isentropic flow expansions to supersonic speeds, leading to very low pressures around the suction peak. Therefore, the RAE 2822 section was chosen as its leading edge had the smallest radius among the three available sections. A maximum thickness of 12% was chosen as the C_p curve just touches the critical C_P line, C_P*. The aerofoil is adjusted until the final design shown in *Figure 1*.

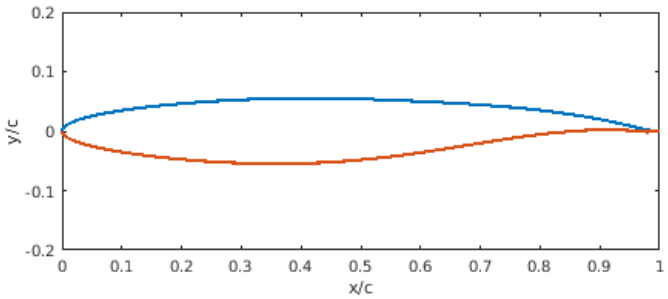

Figure 1: Geometry of my transonic aerofoil section

The leading-edge radius has been kept small as explained in the previous section. This expands the flow at the upper surface leading-edge, thus obtaining more lift than a larger radius. The front half of the upper surface was made to have low curvature, as "flat" as possible. This maintains the supersonic flow and prevents the flow from accelerating further, by restricting more expansion waves from forming. Isentropic recompression waves slow the flow down. The shock is there to bring the flow back to subsonic speeds. Therefore, by having a slower flow enter the shock, the relative strength of the shock has been reduced which reduces wave drag. Lastly, aft camber has been added. This produces more lift in the rear parts of the aerofoil as the pressure increases substantially in the lower surface here. Without aft camber, the majority of lift would be in the front half of the aerofoil, thus rear camber trims this out. However, because of the recompression to satisfy the Kutta condition, camber could lead to an increased adverse pressure gradient which could result in trailing edge separation. Camber also increases drag. Therefore, a compromise has been made for the amount of rear camber applied.

Table 1: Aerofoil conditions and performance metrics at design point

M	Re	α	C_L	C_D	C_{D2}	$\bar{H}_{TE}$	x_{shock}/c
0.73	9.00E+06	2.35°	0.671	0.00859	0.00099	2.146	0.364

Table 1 shows the performance of the aerofoil at its design point, which is at an incidence of $\alpha = 2.35°$. All the design constraints have been met, most notably boundary layer transitioning at $x = 0.05c$ which has been pre-set, a wave drag $C_{D2} \leq 0.0012$ (equivalent to 12 counts), and $\bar{H}_{TE} \leq 2.2$. This gives a satisfactory $C_L/C_D = 78.1$.

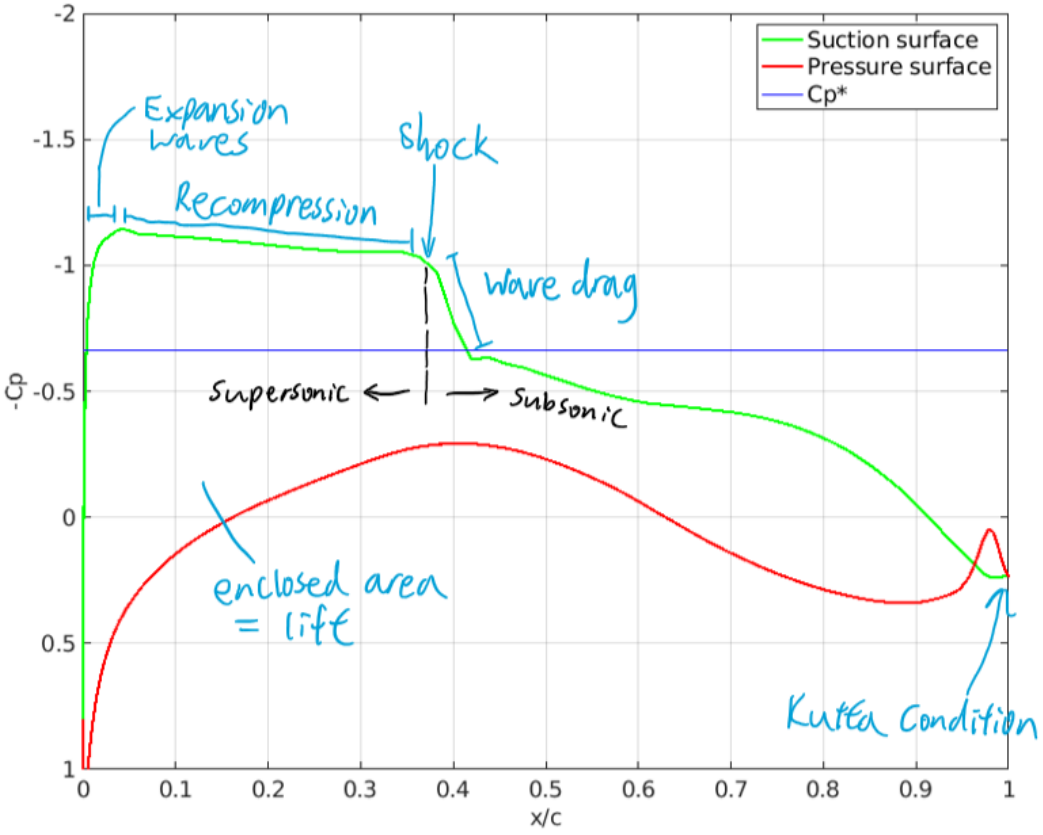

Figure 2: Annotated pressure distribution at design point

The pressure distribution in *Figure 2* shows a few notable features. Firstly, the flow becomes supersonic just past the leading edge, then experiences isentropic recompression throughout the 'pressure plateau'. The flow slows down as a result and enters a relatively weak shock at $x = 0.364c$. Downstream of the shock the flow becomes subsonic, as is the flow throughout the pressure surface. The maximum local Mach number is $M = 1.22$ at $x = 0.042c$ which corresponds to the suction peak. As pressure is directly related to the local Mach and stagnation pressure, the local surface Mach distribution follows exactly the shape of the pressure distribution. Secondly, there is high loading on the rear, subsonic half of the aerofoil. This is seen in the rise in pressure in the lower surface and the 'bulge' in the upper surface, leading to a large enclosed area in the rear of the aerofoil which corresponds to high rear lift. This is ideal as that allows us to trim and balance the lift in the front half of the aerofoil. Thirdly, the pressure

curves cross over briefly at the trailing edge. This is due to the aerofoil designer not allowing the section to have an angled/deflected trailing edge, leading to an unwanted reverse curvature in order to have a zero-angled trailing edge. In other words, there is a point of inflection just in front of the trailing edge and the pressure abruptly increases on the upper surface and vice versa for the lower surface. Lastly, $\bar{H}$ values are below 2.2, implying that the flow has not separated, despite the moderate adverse pressure gradient seen in the pressure distribution. Kutta condition implies flow on both surfaces exit at the trailing edge smoothly, this is seen where the pressures curves meet at $x = c$.

3. Improvements

Ideally the upper surface should have zero curvature, as that prevents more expansion waves from forming and the shock would be weaker as a result. This was not the case as seen in *Figure 1*, because the program only allows the camber of the aerofoil to be varied. This means the aerofoil thickness distribution is fixed. For instance, pushing the upper surface down to make it flat would only cause the lower surface to have excess unwanted curvature, which not only causes very low pressures there but also lower surface flow separation. A compromise was made between how 'flat' the upper surface is and the lower surface curvature. This is unlikely to be 'fixable' unless the program allows editing both surfaces separately.

The leading edge radius could be reduced further to create stronger expansion waves, faster supersonic flows and lower pressures just past the leading edge. This was not possible due to the constraints of the program again, where the leading edge radius is fixed, and since the smallest radius amongst the three starting aerofoils was chosen, this could not be reduced anymore. This problem again could only be solved if individual points could be altered separately, rather than the whole camber with the thickness distribution fixed.

Lastly, the cross-over of pressure curves at the trailing edge was due to the program not allowing the trailing edge to be at an angle. This leads to a slight decrease in lift and a risk in flow separation. This was minimised by having another edit point very close to the trailing edge point, which shifts the point of inflection hence the cross-over as aft as possible. This is unfixable unless the constraint of a zero-angle trailing edge is removed.

Moreover, if the shock could be moved aft, then the lift would increase. However, the position of the shock is closely related to its strength, by moving it aft there is usually a penalty of increased wave drag. By addressing all the above issues, one might see an ideal pressure distribution in *Figure 3.* Given more time/effort, one could mitigate the above issues by fine tuning the curvature in both the supersonic and subsonic surfaces. Increasing the rear camber could lead to increased lift as seen in *Figure 3*, but trailing edge separation occurs. More time could be spent finding a compromise between these aspects of my aerofoil.

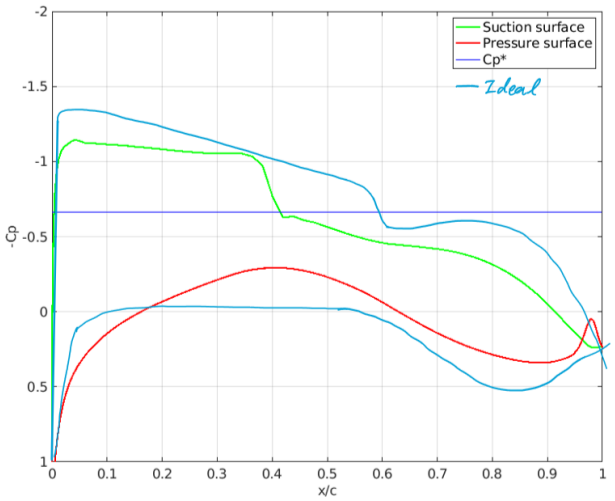

Figure 3: Ideal pressure distribution to maximise lift

4. Off Design

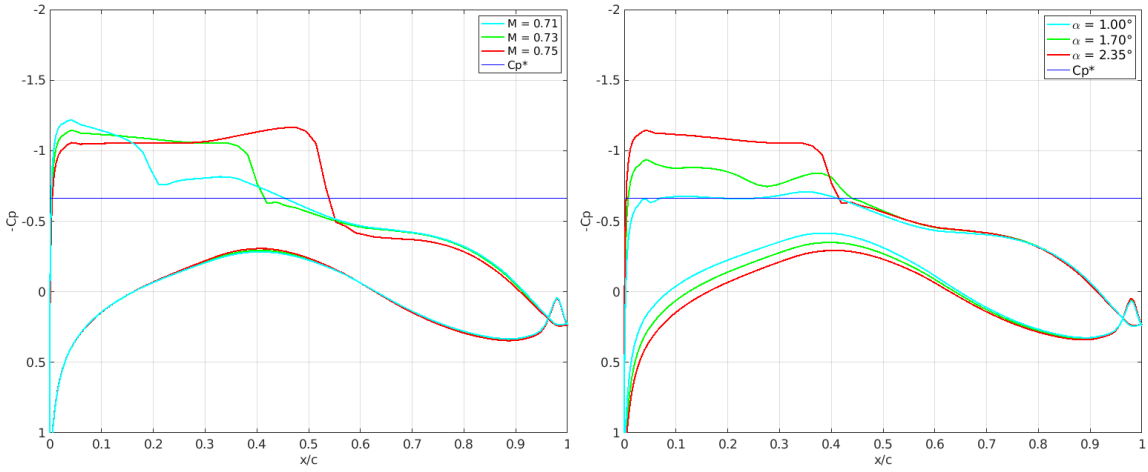

Figure 4: Pressure distributions with varying Mach and incidence

By varying the incidence or Mach number, a similar trend is seen. At a lower angle or Mach, the flow accelerates to a slower velocity just upstream of the shock, leading to the shock weakening and moving upstream. The difference between the two cases is that varying the Mach number has only a small change to the suction peak pressure and has minimal change to the pressure surface pressure distribution. On the other hand, decreasing the incidence reduces lift by changing both surfaces' pressures. The pressure distribution behind the shock does not vary much between the cases, as the shock recompresses the flow to similar conditions.

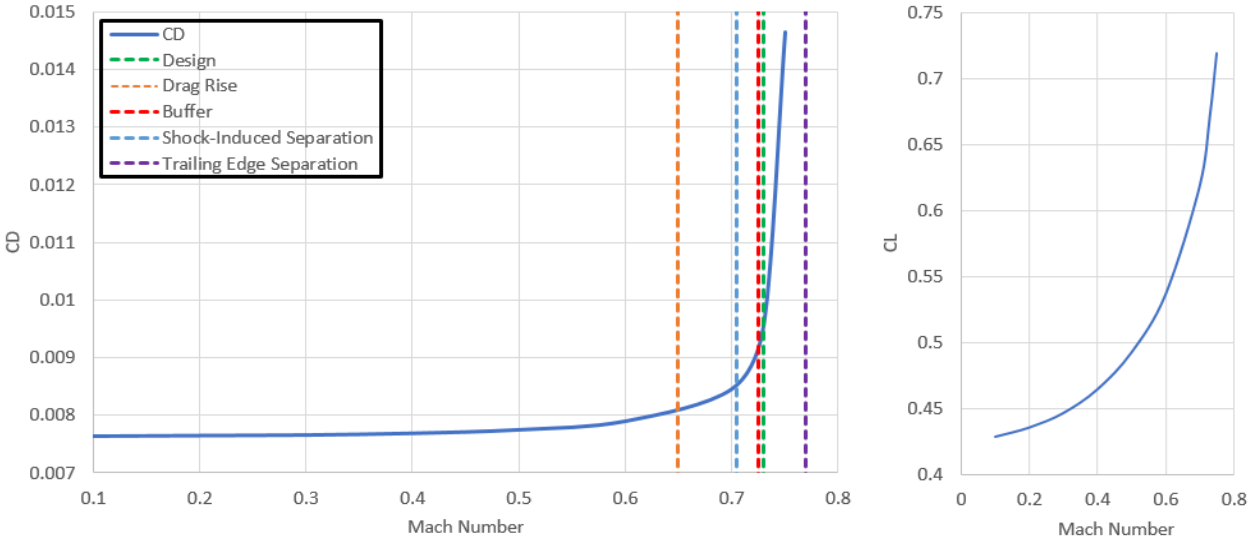

Figure 5: Drag and lift with varying Mach number

When varying Mach number, the drag rise boundary is at $M = 0.65$, this is the point where CD2, the wave drag, first becomes non-zero and the shock to first form on the upper surface. Beyond this point, the drag increases drastically. The buffet onset boundary is at $M = 0.725$. This was identified in *Figure 7*, where the location of shock suddenly moves up and downstream again, an indication of buffet occuring. However, the design point surface mach number plot in *Figure 8* lies beneath all buffet lines (joining 1.5 at the LE to 1.2 at the TE), which suggests the design point is very far from buffeting, so a judgement has been made which priorities the shock position oscillation in *Figure 7*. The onset of shock-induced separation was

identified to be at $M = 0.705$. The minimum local Mach just ahead of the shock which induces separation downstream was estimated to be $M_{local} \approx 1.2$. Therefore, $M = 0.705$ is the point in which the maximum local Mach number just reaches 1.2. Another indication is a 'bulge' in the pressure curve, as a separation bubble has low pressures. The onset of trailing edge separation was unable to be identified. This is because the indication for that is $\bar{H}_{TE} > 2.2$. However, all collectetable data has $\bar{H}_{TE} < 2.2$, as the VGK solver crashes beyond $M = 0.75$ for this aerofoil design. Another indication is C_P drift at the trailing edge, but that was not present too. Plotting $\bar{H}_{TE}$ against Mach number in *Figure 10* in the Appendix this boundary was estimated using extrapolation, which occurs at $M = 0.77$.

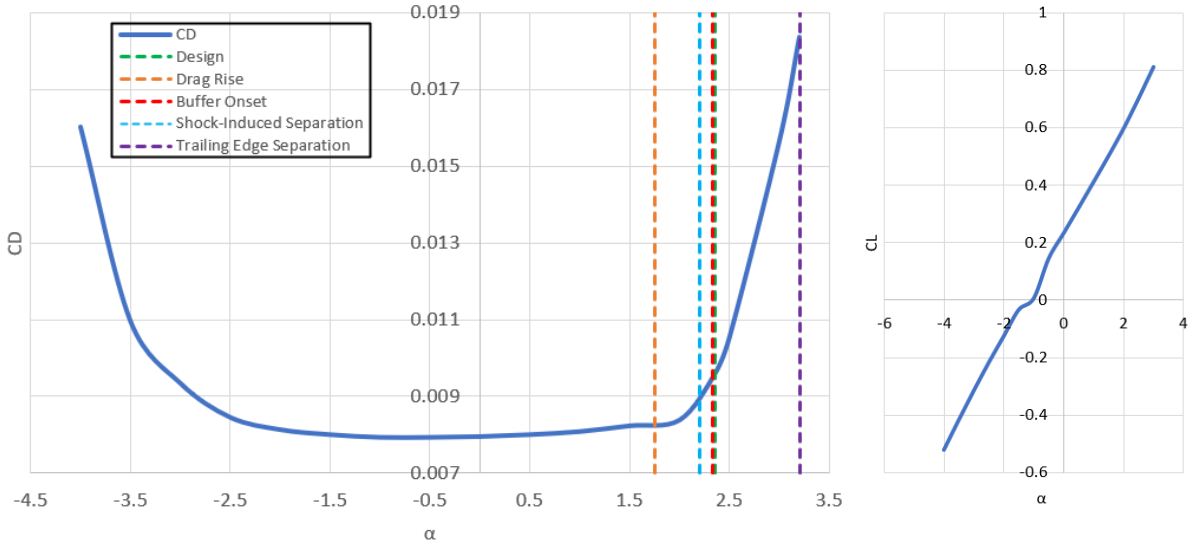

Figure 6: Drag and lift with varying incidence

When varying incidence angle, the same methods are used for identifying all boundaries as varying Mach above. The drag rise boundary is at $\alpha = 1.75°$. The buffer onset boundary is at $\alpha = 2.35°$. This was identified in *Figure 7*, where shock moves up and downstream, an indication of buffet occuring despite surface Mach plot lying under buffet lines. This is in fact the same angle chosen as the design point. The onset of shock-induced separation was identified to be at $\alpha = 2.2°$. The onset of trailing edge separation was unable to be identified as with varying Mach number. The reason is the same as above, where the program crashes above $\alpha = 3.2°$, and $\bar{H}_{TE} < 2.2\ for\ all\ data$. With similar extrapolation from *Figure 10* in the Appendix this is estimated to occur at $\alpha = 3.21°$.

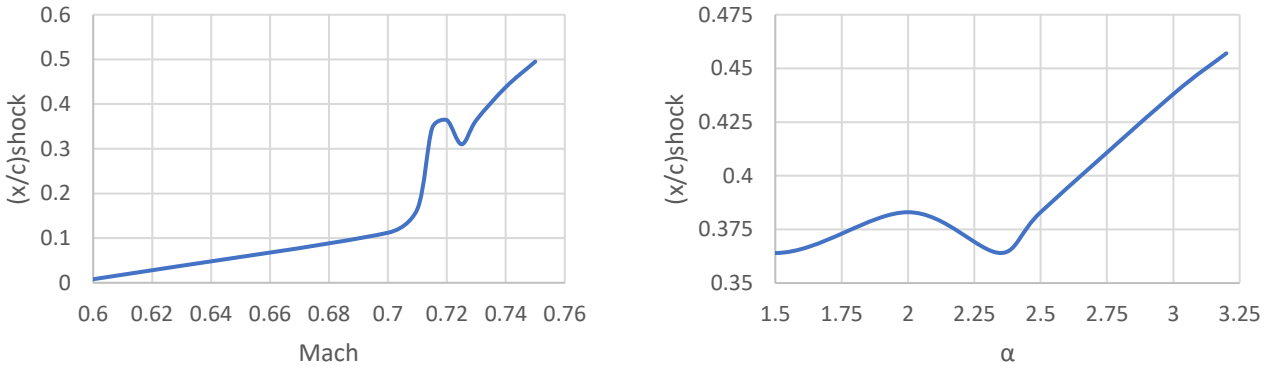

Figure 7: Location of shock varying Mach and incidence

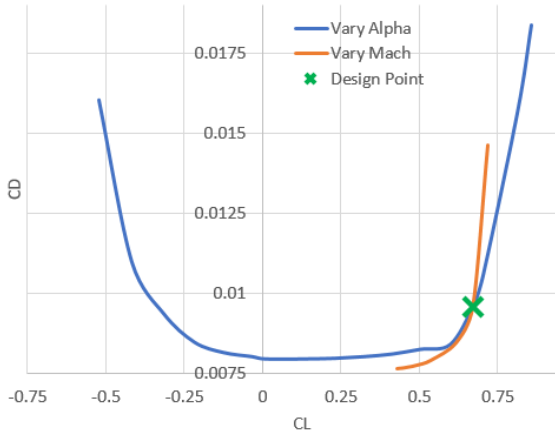

Figure 9: Polar CD-CL plot

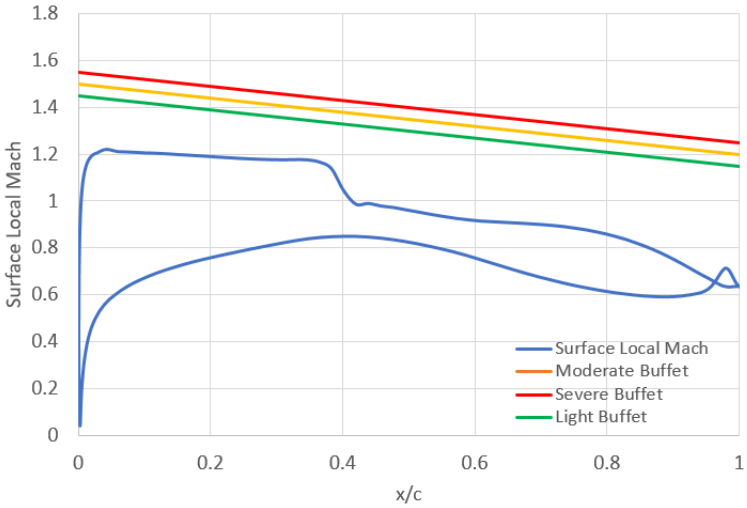

Figure 8: Local surface Mach with buffet lines

Although the design point leads to a good C_L and satisfies all constraints, it is beyond the point of both the onset of shock-induced separation and buffeting. The surface local Mach curve lies below the buffet lines, but this is disregarded due to spotting the oscillation of shock positions. This could mean at the design point our aerofoil could become unstable, either leading to a formation of a separation bubble behind the shock, or unsteady buffeting, where the shock oscillates back and forth in location and strength. Given more time, a design point at below $M = 0.7$ and $\alpha = 2°$ should be chosen and optimised to avoid these boundaries.

5. VGK Solver

The Viscous Garabedian and Korn method is a CFD method coded in FORTRAN that predicts a 2D aerofoil's aerodynamic characteristics and performance metrics in subsonic freestream, but also includes effects of boundary layers, wake and most importantly for this exercise, shock waves. VGK solves finite-difference equations for the inviscid flow region though iterations, which is a potential flow method. The viscous regions are solved using boundary layer integral equations. The solver is able to output the lift, pressure distributions, both inviscid and viscous drag, moments, and most notably the wave drag as a result from the shock wave. The latter is done through a first-order method (CD1), or an improved method (CD2).

However, the solver is limited in predicting trailing edge separation, shock-induced separation bubbles and buffeting. The iterative process may diverge and crash the code which suggests separation or buffeting and does not give any useful results. Other times, these phenomena may happen without crashing. Extra care must then be taken to inspect data such as the shape factor $\bar{H}$ which indicates how 'distressed' the flow if. An excess of 2.2 suggests separation has occurred which the solver does not identify. Sometimes the trailing edge $\bar{H}$ is less than 2.2, but is greater than 2.2 further upstream which shows the limitation of this solver. Similarly, a local Mach > 1.2 ahead of the shock suggests separation behind the shock. This separation bubble and the trailing edge separation can connect, leading to stall. Moreover, the aerofoil shape designer has limitations which were discussed in Section *3. Improvements*.

6. Conclusion

At the aerofoil's design point, a satisfactory lift is maximised to $C_L = 0.671$ while satisfying the boundaries prescribed by wave drag and the trailing edge boundary layer state. Its off-

design performance was evaluated by varying the Mach number and incidence separately. An operational envelope was created through plotting how C_L and C_D varies, where the boundaries for drag rise, buffet, shock-induced and trailing edge separation were identified. As a result, it was found that the design point is beyond the onset of buffeting and shock-induced separation. Even though the surface Mach curve lies below the buffet line joining M=1.5 and 1.2, the oscillation of shock location was considered more significant in identifying buffeting. These suggest the design point could be shifted down to avoid these unstable effects. Improvements could be made to the aerofoil but the section designer program limits this in various ways.

Appendix

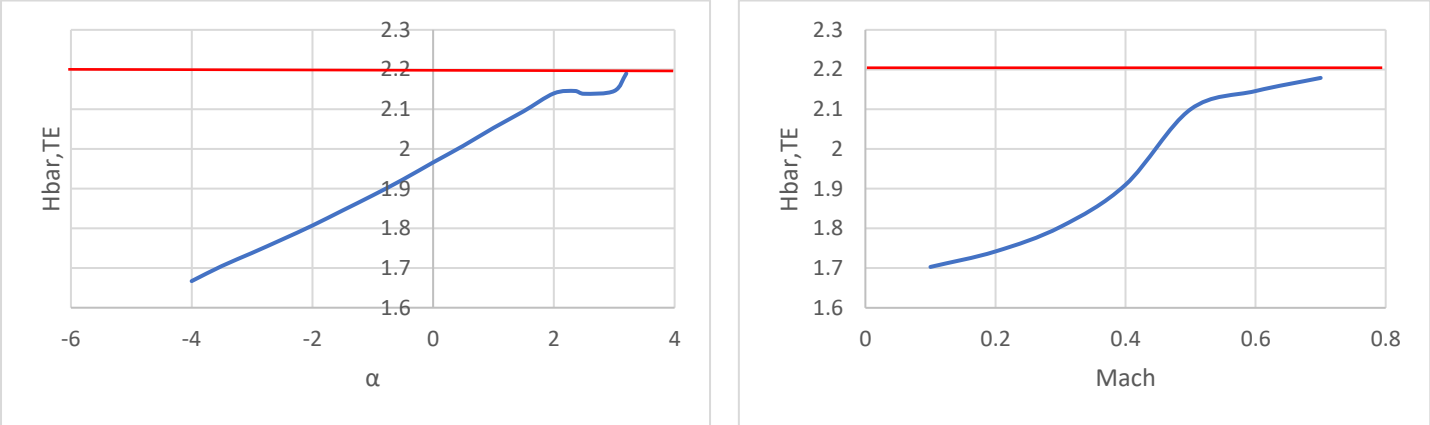

Figure 10: Hbar,TE against incidence and Mach (limit of 2.2 shown in red)

Listing of run.dat file:

Title
0 65 65 0.0 1.0
0.000000 0.000000
0.000600 0.002870
0.002410 0.005732
0.005410 0.008566
0.009610 0.011372
0.014980 0.014143
0.021530 0.016872
0.029230 0.019557
0.038060 0.022198
0.048010 0.024784
0.059040 0.027313
0.071140 0.029776
0.084270 0.032168
0.098400 0.034481
0.113490 0.036710
0.129520 0.038843
0.146450 0.040877

0.164220 0.042805
0.182800 0.044631
0.202150 0.046340
0.222210 0.047942
0.242950 0.049421
0.264300 0.050783
0.286220 0.052002
0.308660 0.053077
0.331560 0.053973
0.354860 0.054661
0.378510 0.055112
0.402450 0.055329
0.426630 0.055309
0.450990 0.055054
0.475470 0.054588
0.500000 0.053930
0.524530 0.053111
0.549010 0.052161
0.573360 0.051119
0.597540 0.049999
0.621490 0.048826
0.645140 0.047583
0.668450 0.046232
0.691340 0.044766
0.713780 0.043173
0.735700 0.041426
0.757050 0.039525
0.777780 0.037469
0.797850 0.035256
0.817200 0.032900
0.835780 0.030405
0.853550 0.027792
0.870480 0.025093
0.886510 0.022309
0.901600 0.019486
0.915740 0.016643
0.928860 0.013836
0.940960 0.011084
0.952000 0.008439
0.961940 0.005946
0.970770 0.003643
0.978470 0.001661
0.985020 0.001076
0.990390 0.000681
0.994590 0.000382
0.997590 0.000168
0.999400 0.000041
1.000000 0.000000
0.000000 0.000000
0.000600 -0.002870
0.002410 -0.005732

0.005410 -0.008566
0.009610 -0.011372
0.014980 -0.014143
0.021530 -0.016873
0.029230 -0.019565
0.038060 -0.022229
0.048010 -0.024857
0.059040 -0.027451
0.071140 -0.030001
0.084270 -0.032505
0.098400 -0.034953
0.113490 -0.037337
0.129520 -0.039638
0.146450 -0.041846
0.164220 -0.043941
0.182800 -0.045913
0.202150 -0.047737
0.222210 -0.049414
0.242950 -0.050914
0.264300 -0.052232
0.286220 -0.053329
0.308660 -0.054189
0.331560 -0.054765
0.354860 -0.055012
0.378510 -0.054888
0.402450 -0.054381
0.426630 -0.053474
0.450990 -0.052157
0.475470 -0.050443
0.500000 -0.048340
0.524530 -0.045871
0.549010 -0.043060
0.573360 -0.039942
0.597540 -0.036529
0.621490 -0.032897
0.645140 -0.029145
0.668450 -0.025345
0.691340 -0.021597
0.713780 -0.017977
0.735700 -0.014537
0.757050 -0.011342
0.777780 -0.008438
0.797850 -0.005856
0.817200 -0.003625
0.835780 -0.001750
0.853550 -0.000239
0.870480 0.000886
0.886510 0.001653
0.901600 0.002064
0.915740 0.002155
0.928860 0.001955

0.940960 0.001519
0.952000 0.000890
0.961940 0.000124
0.970770 -0.000727
0.978470 -0.001491
0.985020 -0.001076
0.990390 -0.000681
0.994590 -0.000382
0.997590 -0.000168
0.999400 -0.000041
1.000000 0.000000